

## SURFACE MODIFICATION OF SILICA NANOPARTICLES BY MEANS OF SILANES: EFFECT OF VARIOUS PARAMETERS ON THE GRAFTING REACTIONS

O. Bounekta<sup>1,2</sup>, R. Doufnoune<sup>1,2\*</sup>, A. Ourari<sup>3</sup>, F. Riahi<sup>4</sup>, N. Haddaoui<sup>5</sup>

<sup>1</sup>URMES, Equipe de Valorisation des Polymères, Université Ferhat Abbas Sétif-1, Algérie

<sup>2</sup>Département de Génie des Procédés, Université Ferhat Abbas Sétif-1, Algérie

<sup>3</sup>LEIMCR, Faculté de Technologie, Université Ferhat Abbas Sétif-1, Algérie

<sup>4</sup>LMPMP, Faculté de Technologie, Université Ferhat Abbas Sétif-1, Algérie

<sup>5</sup>LPCHP, Faculté de Technologie, Université Ferhat Abbas Sétif-1, Algérie

Received: 21 October 2018 / Accepted: 10 December 2018 / Published online: 01 January 2019

### ABSTRACT

The adsorption of four silanes, namely: N-(2-Aminoethyl)-3-aminopropyltrimethoxysilane (AEAPTMS), 3-methacryloxypropyltrimethoxysilane (MPTMS), allyltrimethoxysilane (ATMS), N-2-[(N-vinylbenzylamino)ethyl]-3-aminopropyltrimethoxysilane hydrochloride (CVBS) onto the surface of silica nanoparticles has been studied using water/ethanol (5/95, v/v) mixture. Four experimental parameters were explored for the grafting of the silanes: pH, concentration, time, and temperature. Possible interactions between the silanes and the surface of silica were investigated by means of FT-IR Spectroscopy. The FT-IR analyses confirmed the effectiveness of the silanization of the silica surface. The amount of the adsorbed silane on the silica nanoparticles appeared to be influenced by the initial concentration of the silane, pH, time and temperature of modification.

**Keywords:** nanoparticles of silica; organosilanes; surface modification; dissolution tests; FT-IR spectroscopy.

Author Correspondence, e-mail: [doufnoune@yahoo.fr](mailto:doufnoune@yahoo.fr)

doi: <http://dx.doi.org/10.4314/jfas.v11i1.14>



## 1. INTRODUCTION

Silica nanoparticles in the crystalline and amorphous forms have been received enormous attention owing to their peculiar and fascinating properties. They offer wide breadth of potential applications in various fields, including heterogeneous supported catalysts, adsorbents and supports for gas and liquid chromatography, biology with its diverse activities, pharmaceutical drugs, cosmetics, electronic and optic devices, automotive, appliance, consumer goods, aerospace and sensor industries. Silica nanoparticles have been also used as nanofillers in the rubber products, and plastics binders for improving the thermal resistance, electrical and mechanical properties [1-6]. In all of these applications a proper interfacial interaction is needed to ensure a good dispersibility and stability of the nanoparticles in various liquid media. Therefore the interface between the particles and the media in which they are incorporated plays an important role [7-9].

The chemical properties of the silica surface are mainly determined by the density of silanol per gram of silica. At the surface, the structure terminates in either a siloxane group (Si-O-Si) with the oxygen on the surface, or one of several forms of silanol groups (Si-OH). The silanol groups can be divided into: (i) isolated groups (single silanols); (ii) vicinal silanols (or bridged silanols), or OH groups bound through the hydrogen bond (H-bonded single silanols, H-bonded geminals, and their H-bonded combinations); and (iii) geminal silanols, geminal free (geminal silanols or silanediols) [10-12].

The silanol groups can be easily functionalized by various chemical procedures. Generally, the most effective technique is the use of the reaction of silanol groups with suitable organosilane agents. Their general formula is  $R_nSiX_{4-n}$ , where  $n$  may be varied between 1 and 3 whereas the  $X$  is a hydrolyzable group typically three methoxy, ethoxy, or isopropoxy groups. Following hydrolysis, a reactive silanol group is formed, which can condense with the silanols present on the silica surface to form siloxane linkages. The  $R$  group is a non-hydrolyzable organic radical that may possess a functionality that imparts desired characteristics [13-17].

Most of the widely used organosilanes have one organic substituent and three hydrolyzable substituents. In the vast majority of surface treatment applications, the alkoxy groups of the

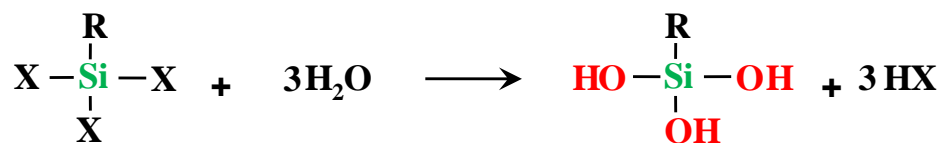
---

trialkoxysilanes are hydrolyzed by water present in the liquid phase or at the substrate surface to form silanol-containing species followed by the chemisorption process to the surface. Hydroxyl groups present on the surface were believed to interact with the hydrolyzed silane molecules via hydrogen bonds. Finally, during drying or curing, a covalent linkage is formed with the substrate with a concomitant loss of water (see simplified descriptive reactions in Figure 1) [18-24].

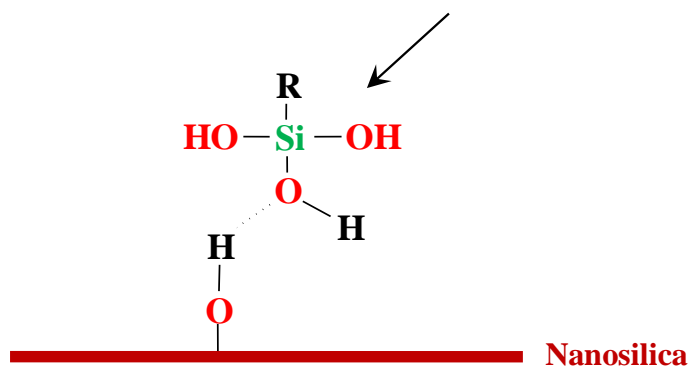
Commonly, two different ways are employed for depositing an organosilane on a surface. In the extreme, there is: (i) the dry treatment, in which the silica particles are mixed with the silane under anhydrous conditions, and (ii) the wet or slurry treatment, where the silane is deposited from an aqueous solution. The above procedures can lead to silica surface of greatly differing properties. In the case of wet treatment, several parameters in the silanization process are investigated, for instance the effects of temperature, silane concentration, time and solvent. The pH of the aqueous slurry and catalytic substances for the silanization process have also been reported [25-30].

The incorporation of nanosilica as a nanofiller into a polymer matrix seems to be not easy. This is essentially due to the very small dimensions, large specific area, and high surface free energy. Consequently, the silica nanoparticles tend to agglomerate to form larger particles. Hence, the final physical and mechanical properties of the polymeric nanocomposites will be reduced. The surface modification of silica prior to mixing is a practical method to improve not only the dispersion but also to compatibilize the nanofiller with the polymeric matrix. In this method, compatible functional groups typically methacryloxy, isocyanate, epoxy, amino, mercapto, vinyl, allyl etc... with the chemical structure of the polymer matrix are grafted on the surface of the silica [29, 31-35]. Due to the large surface area to volume ratio of the nanoparticles as well as the use of silylated nanoparticles, the microstructure and properties of the polymer matrix is altered at the nanoparticles/matrix interface and the amount of this perturbed zone, referred to as interphase, could be important. But it is largely accepted that the interphase can notably affect the performance of nanocomposites, the reported interphase property and thickness vary from case to case [36].

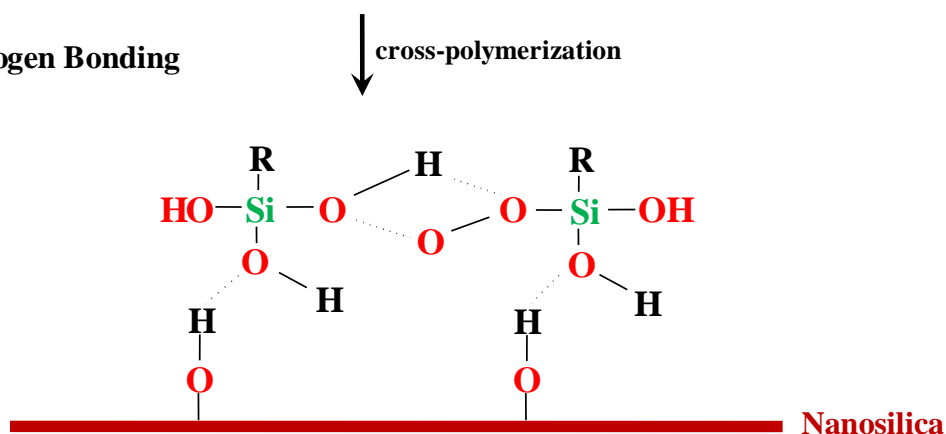
## 1/ Hydrolysis



## 2/ Chemisorption



## 3/ Hydrogen Bonding



## 4/ Bond Formation

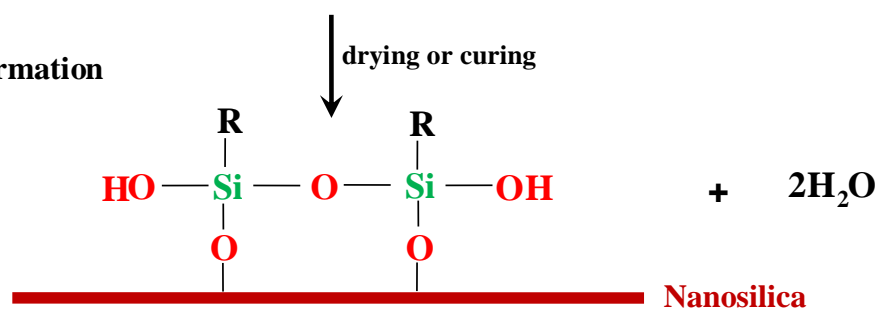


**Fig.1.** Adsorption of silanes onto nanosilica particles

In this study, four silanes presenting different functionalities were chosen to modify the surface of the silica: (i) N-(2-Aminoethyl)-3-aminopropyltri-methoxysilane (AEAPTMS), (ii) 3-methacryloxypropyltrimethoxysilane (MPTMS), (iii) allyltrimethoxysilane (ATMS) and (iv) N-2-[(N-vinylbenzylamino)ethyl]-3-aminopropyltrimethoxysilane hydrochloride (CVBS). The effect of pH value, silane concentration, reaction time and temperature on the chemical

modification of silica nanoparticles was investigated. Dissolution test and Fourier transform infrared spectroscopy (FT-IR) were used as the characterization methods for the silane-modified silica nanoparticles.

## 2. EXPERIMENTAL

### 2.1. Materials

Amorphous silica, referenced as (CAS No S5130) was supplied from Sigma-Aldrich. Its physico-chemical characteristics are given in Table 1. N-(2-aminoethyl)-3-propyltrimethoxysilane amino (AEAPTS), 3-methacryloxypropyltrimethoxysilane (MPTMS), allyltrimethoxysilane (ATMS) and N-2-(N-vinylbenzylamino)ethyl-3-aminopropyl trimethoxysilane hydrochloride (CVBS) were purchased from Sigma-Aldrich and Dow Corning Inc., respectively. Figure 2 shows the chemical structures of the corresponding silanes. Solvents such as ethanol, methanol, cyclohexane and tetrahydrofuran (THF) were purchased from Merck Chemicals Ltd. In addition, 0.1 mol/L of acetic acid and sodium hydroxide solutions were used to adjust the pH value. All chemicals were used as received without any further purification.

**Table 1.** Characteristics of nano-silica

Properties	Values
Density (g/cm <sup>3</sup> )	2.3
Particle size (µm)	0.007
Specific surface area (m <sup>2</sup> /g)	395 ± 25
pH (at 4%)	3.7-4.7
Purity (%)	99.8

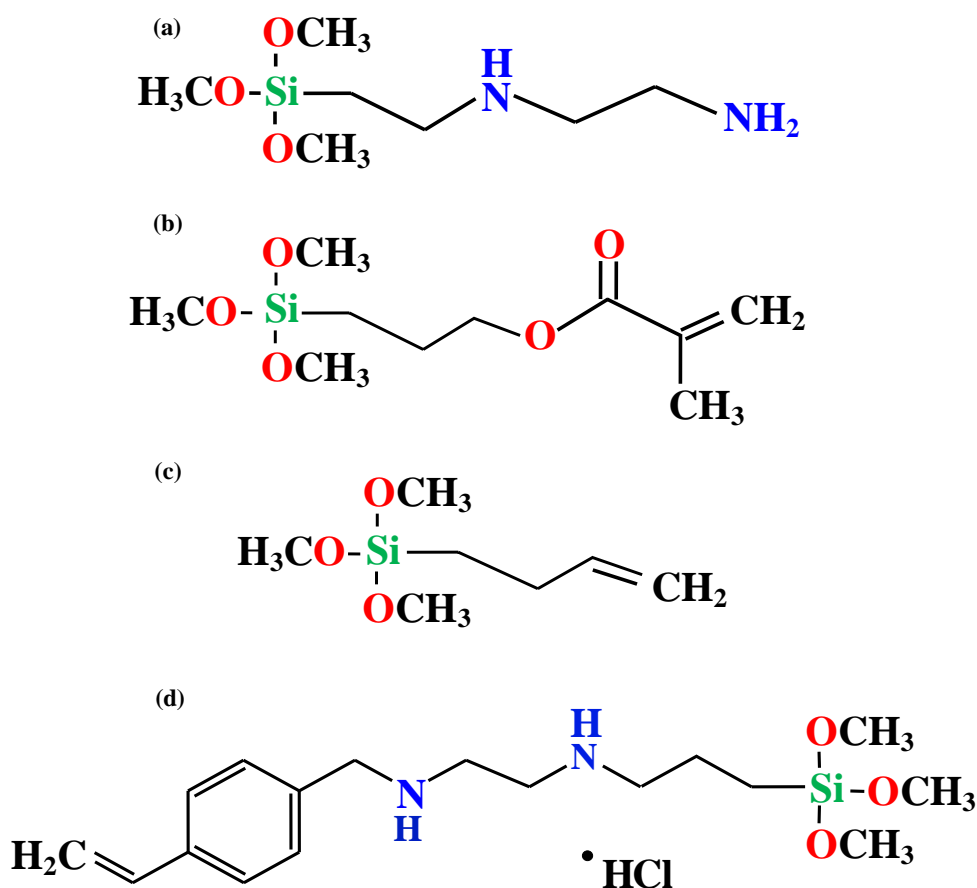


**Fig.2.** Chemical formulas of silane molecules: (a) AEAPTMS, (b) MPTMS, (c) ATMS and (d) CVBS

## 2.2. Surface modification of silica nanoparticles

All of the silica treatment experiments involved a solution method: In a typical experiment, each silane was hydrolyzed for about 30 min and dissolved in 250 ml of ethanol/water mixture (95/5 v/v). The pH of the mixture was adjusted to the required value with acetic acid or sodium hydroxide. A Mettler Toledo<sup>TM</sup> model S220 digital pH meter equipped with a standard glass was used to determine the pH values. The modified silica was filtered over a Büchner-funnel, washed with THF and then was slowly dried under air at room temperature to improve the stability of the coating and then cured for 1 day in an oven at approximately 105 °C to complete the condensation process and the formation of polysiloxane network structures. In all experiments time zero was taken as the moment when silica nanoparticles were added to the

hydrolyzed silanes. In addition, the initial concentration of the silane in solution was calculated as the weight percent of silane on silica. The synthesized silane-modified silica nanoparticles were denoted as AEAPTMS-SiO<sub>2</sub>, MPTMS-SiO<sub>2</sub>, ATMS-SiO<sub>2</sub> and CVBS-SiO<sub>2</sub>.

### 2.3. Determination of silane adsorption by the dissolution test

The amount of silane adsorbed on the silica surface was determined by a dissolution test according to the research work reported by Demjén et al. [37]. The sample was stirred in 100 ml cyclohexane for 30 min and then left standing for 1 day. The suspension was centrifuged for 10 min at 6000 cm<sup>-1</sup>. The concentration of the solution was determined by FT-IR spectroscopy and the amount of silane coupled permanently to the surface of silica was calculated. The dissolution of aminosilane (AEAPTS) adsorbed onto the silica was exceptionally conducted in methanol. The structure of the adsorbed silane derivatives was determined before and after washing with THF using FT-IR spectroscopy.

### 2.4. Fourier Transform Infra-Red Spectroscopy (FT-IR)

The infrared spectra were recorded at room temperature with a Perkin Elmer FT-IR spectrometer. The spectra of the grafted products were obtained in transmission using the KBr plate method. About 5 mg of particles were mixed with 95 mg of potassium bromide. The extracts were deposited as a drop on KCl window after evaporation of the solvent. The spectra in transmission mode were recorded in a range from 4000 to 400 cm<sup>-1</sup>, after 132 scans with a resolution of 4 cm<sup>-1</sup>.

## 3. RESULTS AND DISCUSSION

Figure 3 shows the FT-IR spectra of the neat silica nanoparticles. The broad bands between 3750 and 3000 cm<sup>-1</sup> are attributed to the physisorbed water and to the silanol groups of silica surface (vicinal OH). This broad band is due to the intermolecular interactions of water hydroxyls, whereas the vicinal silanols induce in the same region inter- and intramolecular interactions commonly known as bonded hydrogen. The sharp absorption band observed at 3752 cm<sup>-1</sup> is ascribed to the free hydroxyl groups, and the weak band observed at 963 cm<sup>-1</sup> is assigned to the surface free Si-OH groups (isolated and geminated OH). The absorption band seen at 1637 cm<sup>-1</sup> is assigned to the adsorbed water molecules with their hydroxyl groups. As

for the strong band, observed at  $1085\text{ cm}^{-1}$ , it is also assigned to Si-O-Si asymmetric stretching vibration and the absorption bands appearing at  $806$  and  $465\text{ cm}^{-1}$  are attributed to Si-O-Si and Si-O symmetric stretching vibration and bending mode, respectively [29,38].

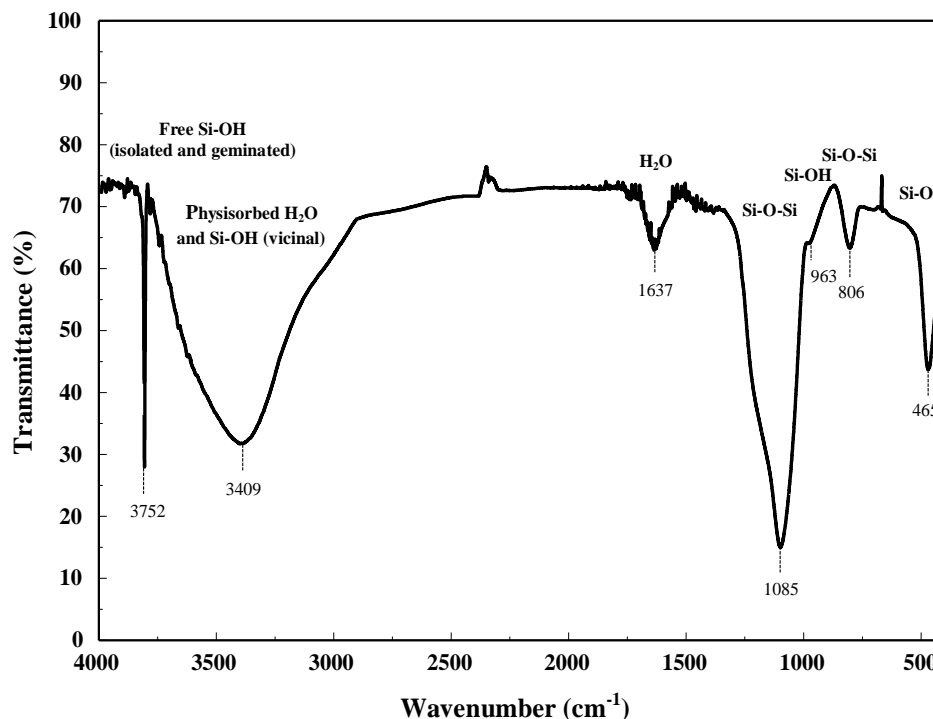


**Fig.3.** FT-IR spectrum of the unmodified silica nanoparticles

The FT-IR spectra of pure AEAPTMS, MPTMS, ATMS and CVBS are presented in Figure 4. The assignment attempts of the absorption bands of these four compounds are listed in Table 2. The pure AEAPMS (Figure 4a) displays two weak absorption bands, between  $3375$  and  $3291\text{ cm}^{-1}$ . These two bands were ascribed to the free amine asymmetrical and symmetrical N-H stretching modes, respectively. The N-H bending vibration of primary amines was rather observed at  $1576\text{ cm}^{-1}$ . As for the hypothetic four bands which should be seen between  $3000$  and  $2800\text{ cm}^{-1}$ , they are assignable to the two successive asymmetric and symmetric stretching modes of methyl ( $\text{CH}_3$ ) and methylene ( $\text{CH}_2$ ) groups, describing the hydrophobic entities of the AEAPTMS molecules. In this case, the doublet expressing the presence of methylene groups is clearly observed, while the second appears only as shoulders just before the two previous bands. The strong absorption band seen at  $1100\text{ cm}^{-1}$  was attributed to the Si-O-C stretching mode of methoxy groups. The absorption bands near  $1454$  and  $1190\text{ cm}^{-1}$  were assigned to the



CH<sub>3</sub> bending and rocking modes, respectively. The very strong band which appeared at 781 cm<sup>-1</sup> was due to the Si-C stretching vibrations.

Concerning the MPTMS (Figure 4b), it showed the same absorption bands for the identical moieties constituting the four compounds studied in this work. For this reason, only the absorption bands characterizing their main differences will be noted like the absorption bands observed at 1714 and 1636 cm<sup>-1</sup>, respectively and were assigned to the C=O functional groups and C=C expressing their stretching vibrations. For the band located at 937 cm<sup>-1</sup>, it may also be considered as the result of the double bond C=C. For the regions where the hydrophobic entities (CH<sub>3</sub>, CH<sub>2</sub>), ether and silicic groups were almost observed around the same values as mentioned above (See Figure 4a and Table 2).

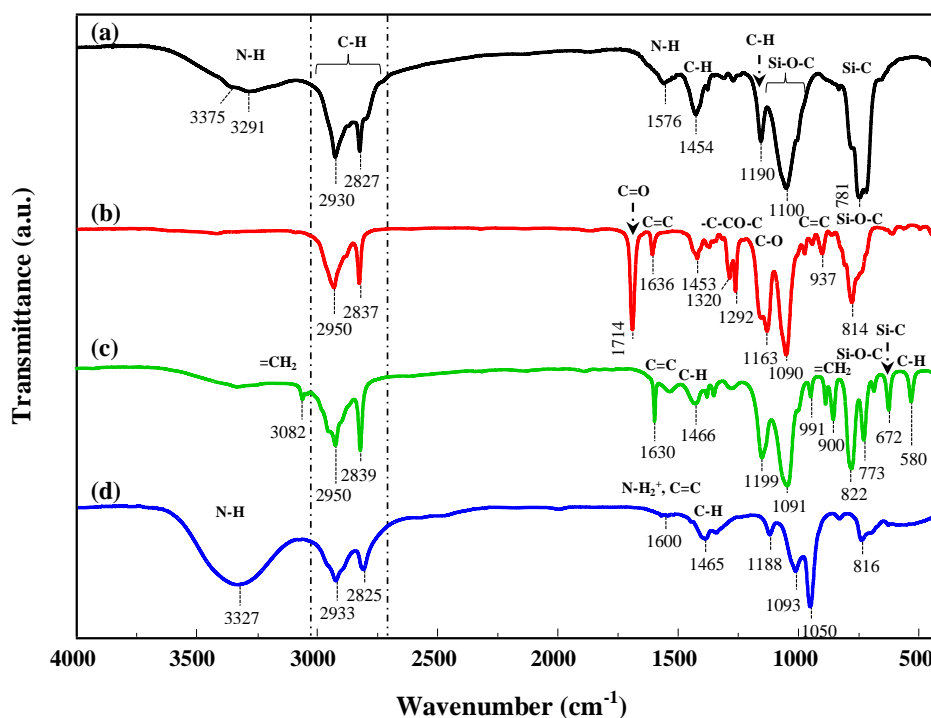


**Fig.4.** FT-IR spectra of pure silanes: a) AEAPTMS, b) MPTMS, c) ATMS and d) CVBS

The spectrum of the pure ATMS (Figure 4c) displays four absorption bands at 3082, 1630, 991 and 900 cm<sup>-1</sup>. These bands may be respectively ascribed to the =CH<sub>2</sub> and C=C asymmetric stretching vibrations, and the two last ones to the CH<sub>2</sub> twisting and wagging modes.

**Table 2.** Frequencies and tentative assignments for silanes used in this study

AEAPTS	assignments	MPTMS	assignments	ATMS	assignments	CVBS	assignments
3375	$\nu_a$ (N-H)	2950	$\nu_a$ (CH <sub>3</sub> )	3082	$\nu_a$ (=CH <sub>2</sub> )	3327	$\nu_a$ (N-H)
3291	$\nu_s$ (N-H)	2837	$\nu_s$ (CH <sub>3</sub> )	2950	$\nu_a$ (CH <sub>3</sub> ) <sub>OCH<sub>3</sub></sub>	2933	$\nu_a$ (CH <sub>3</sub> )
2930	$\nu_a$ (CH <sub>2</sub> )	1714	$\nu$ (C=O)	2839	$\nu_s$ (CH <sub>3</sub> ) <sub>OCH<sub>3</sub></sub>	2825	$\nu_s$ (CH <sub>3</sub> )
2827	$\nu_s$ (CH <sub>2</sub> )	1636	$\nu$ (C=C)	1630	$\nu_a$ (C=C)	1600	$\nu$ (C=C)
1576	$\delta$ (NH <sub>2</sub> )	1453	$\delta_a$ (CH <sub>3</sub> )	1460	$\delta_a$ (CH <sub>3</sub> )	1465	$\delta_a$ (CH <sub>3</sub> )
1454	$\delta_a$ (CH <sub>3</sub> )	1320	$\nu$ (C-CO-C)	1199	$\omega$ (CH <sub>2</sub> )	1188	$\nu$ (C-O)
1190	$\rho$ (-CH <sub>3</sub> )	1292	$\nu$ (C-CO-C)	1091	$\nu_a$ (Si-O-C)	1093	$\nu_a$ (Si-O-C)
1100	$\nu_a$ (Si-O-C)	1163	$\nu$ (C-CO-C)	991	$\tau$ (=CH <sub>2</sub> )	1050	$\nu_a$ (Si-O-C)
781	$\nu$ (Si-C)	1090	$\nu_a$ (Si-O-C)	900	$\omega$ (=CH <sub>2</sub> )	816	$\nu_a$ (Si-O-C)
		937	$\nu$ (C=C)	822	$\nu_a$ (Si-O-C)		
		814	$\nu_s$ (Si-O-C)	773	$\tau$ (CH <sub>2</sub> )		
				672	$\nu$ (Si-C)		
				580	$\delta$ (C-H)		

*Abbreviations:  $\nu$ , stretching;  $\delta$ , bending;  $\tau$ , twisting;  $\omega$ , wagging;  $\rho$ , rocking.*

Regarding the last spectrum of the pure CVBS (Figure 4d), the absorption bands around 3327 cm<sup>-1</sup> indicate the asymmetric NH stretching vibrations with other asymmetric and symmetric displaying systematically some structural similarities. The band around 1600 cm<sup>-1</sup> is ascribed to the asymmetric and symmetric (-NH-) bending modes. The vinyl group and =CH bonds belonging to the aromatic moieties should be observed at higher than 3000 cm<sup>-1</sup>, while the double bonds like those implicated in the electronic delocalization were obviously seen at 1600 and 1465 cm<sup>-1</sup>. For the hydrophobic entities such as those of (CH<sub>3</sub>, CH<sub>2</sub>), ether and silicic groups were as well observed as indicated above due to their structural similarities [39-42].

For the modified silica nanoparticles with different silanes, their FT-IR spectra are presented in Figure 5. After the silanization treatment, the band of the isolated or free hydroxyl groups, habitually observed at 3752 cm<sup>-1</sup> disappeared, while the absorption band, initially observed at 3409 cm<sup>-1</sup> was found to shift to 3450 cm<sup>-1</sup> and accompanied by hypochromic effect. This result

suggests that the physisorbed water molecules and isolated OH groups have effectively reacted with silane molecules. In addition to this, the band of Si-O-Si was shifted from  $1085\text{ cm}^{-1}$  to  $1130\text{ cm}^{-1}$ . This shifting is generally characteristic of a highly condensed siloxane polymer. In this case, it must be noticed that the hydrophobic moieties like  $\text{CH}_3$  and  $\text{CH}_2$  groups may be considered as being the main entities indicating the success of the modification of silica surface. Each one of these moieties was expressed in their spectra by two absorption bands located between  $3000$  and  $2800\text{ cm}^{-1}$  (See Figure 5). Furthermore, some other absorption bands may also be observed for each one of the four cases.

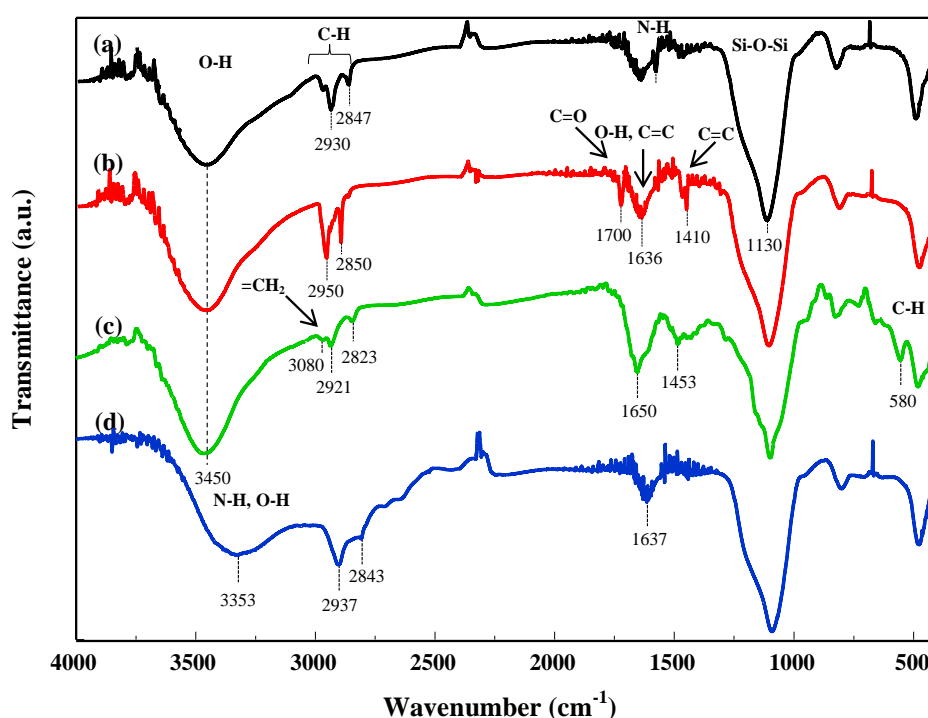


**Fig.5.** FT-IR spectra of the modified silica nanoparticles: a) AEAPTMS-SiO<sub>2</sub>, b) MPTMS -SiO<sub>2</sub>, c) ATMS -SiO<sub>2</sub> and d) CVBS -SiO<sub>2</sub>

The AEAPTMS-SiO<sub>2</sub> (Figure 5a) displays a shifting of the primary amino group from  $1576$  to  $1569\text{ cm}^{-1}$ , confirming the formation of strong hydrogen bonds which were created from the silanol functions and probably containing other contributions obtained from the multilayers by action of the modifier agent. All these results confirm the effectiveness of silanization and are in good agreement with those reported by Culler et al. [39] and Chiang et al. [42] who studied the adsorption of APTES on glass surface as well as Doufnoune et al. [43] who investigated the

adsorption of AEATPMS on  $\text{CaCO}_3$  surface. In this case, it is worthy to note that the results obtained by these authors [39,43] proved that the chemisorbed and physisorbed silanes were formed on the surface of the materials. As well, the same authors demonstrated that the chemisorbed silanes are chemically bonded to the surface via Si-O-Si linkages, while the physisorbed layers are intermolecularly bonded through Si-O-Si bonds.

In Figure 5b which presents the FT-IR spectrum of MPTMS- $\text{SiO}_2$ , the bands located at 1636 and  $1410\text{ cm}^{-1}$  were attributed to C=C stretching of methacrylate and vinyl groups, respectively. The position of the band related to the ester carbonyl groups of methacryloxysilane shifted from 1714 to  $1700\text{ cm}^{-1}$  with MPTMS- $\text{SiO}_2$ . This observation can be explained by the appearance of the intramolecular and intermolecular hydrogen bonds, confirming the high density of the MPTMS- $\text{SiO}_2$  system [44]. Thus, the FT-IR results indicate that the MPMS compound was effectively grafted to the silica nanoparticles. Regarding Figure 5c, illustrating the FT-IR spectra of ATMS- $\text{SiO}_2$ , it was also confirmed that the ATMS compound was grafted on the silica surface. This was proved with the absorption bands observed at 3080, 1650 and  $580\text{ cm}^{-1}$ , which are assigned to the  $=\text{CH}_2$ , C=C and C-H groups, respectively. These bands provided more evidence for the successful silanization reaction.

The FT-IR spectrum of CVBS- $\text{SiO}_2$  is presented in Figure 5d in which the broad bands observed around  $3353\text{ cm}^{-1}$  was ascribed to N-H stretching vibrations. This region includes also the absorption of the O-H groups, confirming the successful grafting of the silane on the surface of the silica.

The structure of the silanes adsorbed on the silica nanoparticles surface was also determined by the FT-IR spectra. The extracted products using THF showed their characteristic absorption bands in the spectral range of  $1400\text{-}900\text{ cm}^{-1}$ . The FT-IR spectrum of the AEAPTMS extracted with THF from silica surface (Figure 6a) shows two bands at 1193 and  $1087\text{ cm}^{-1}$ , which were assigned to the stretching vibrations of the Si-O-Si bond usually observed for materials of high-molecular-weight [43,45]. The very weak band located at  $1041\text{ cm}^{-1}$  is also imputable to the presence of polyaminopolysiloxanes resulting from the condensation of AEAPTMS leading to the formation of an oligomer on the silica surface.

Figure 6b which displays the FT-IR spectrum of MPTMS extracted with THF from silica surface. This Figure exhibits absorption bands at 1188 and 1088  $\text{cm}^{-1}$  characterizing the presence of the Si-O-Si bonds of a highly crosslinked polymeric material. The FT-IR spectrum of the ATMS extracted with THF from the surface of silica (Figure 6c), shows three new bands at 1165, 1105 and 1082  $\text{cm}^{-1}$  indicating the disappearance of the silanol groups of the silane and the formation of polysiloxane. While in the case of CVBS (Figure 6d), the spectrum obtained shows two weak bands at 1128 and 1040  $\text{cm}^{-1}$ , suggesting that these two bands express probably the bulky R groups corresponding to the forms of a low-molecular-weight, cage-like structure on the filler surface [37].

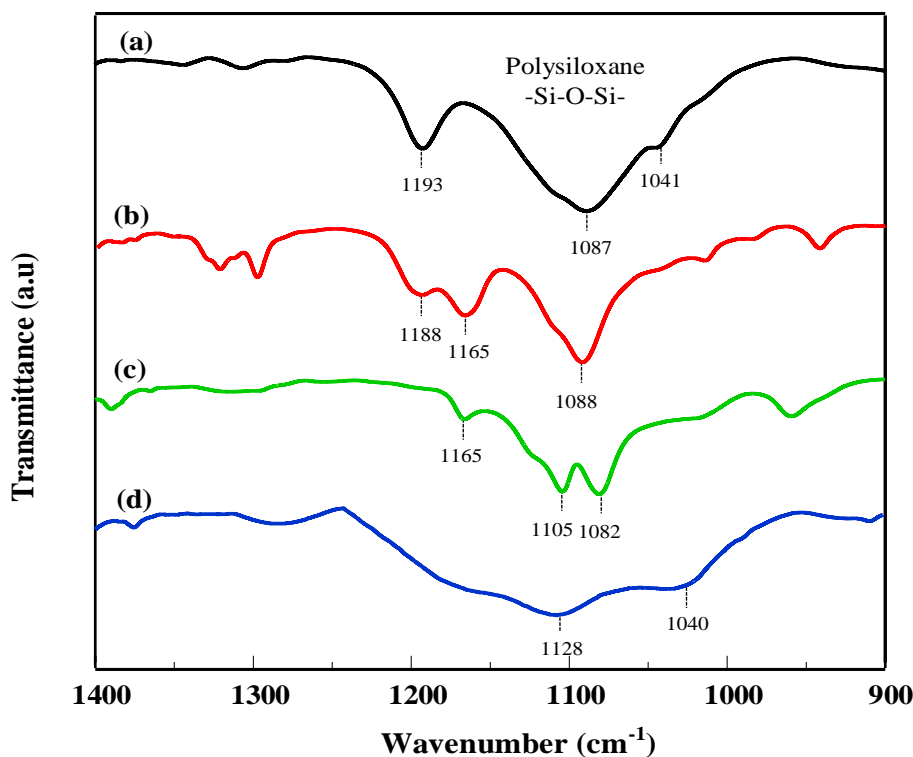


**Fig.6.** FT-IR spectra of: a) AEAPTMS, b) MPTMS, c) ATMS and d) CVBS extracted with THF

## 3.2. Parameters affecting the grafting reactions

### 3.2.1. The effect of the solution pH

The silane adsorption was revealed to be remarkably influenced by the pH as shown in Figure 7, where the amount of the adsorbed silanes is plotted versus the solution pH values. The silica nanoparticles were treated with 10 % silane solutions for 2 h at 60 °C.

The results obtained indicate that all silanes can adsorb onto silica over a wide pH range with the most efficient treatment in the acidic media, whereas in the basic conditions the results seem to be less efficient. Nevertheless, Doufnoune et al. [43], Favis et al. [47] and Plueddemann [48] have concluded that the treatment applied on the  $\text{CaCO}_3$ , mica flakes and glass fiber substrates with different silanes was found to be efficient in a wide range of pH values.

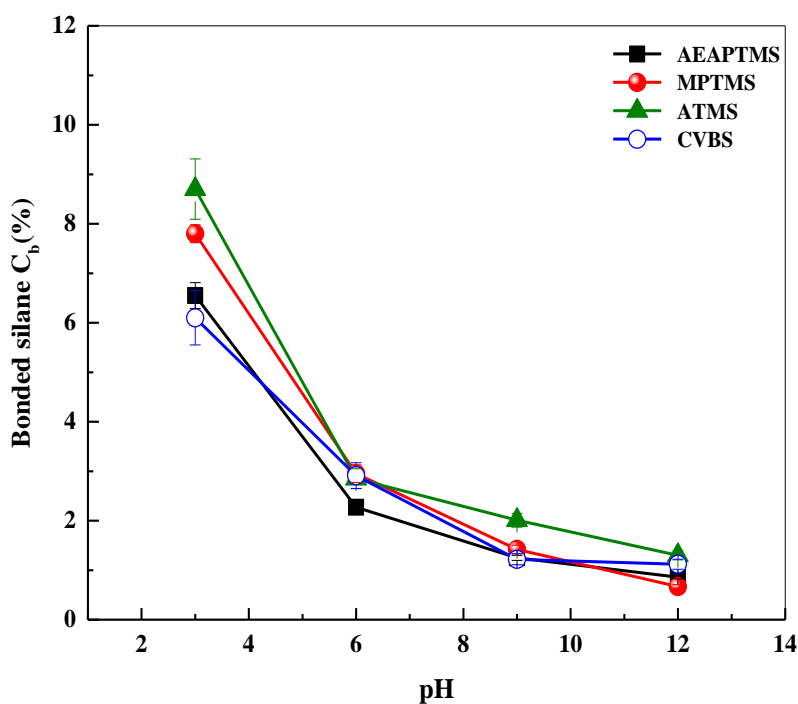


**Fig.7.** Effect of pH on the silane adsorption onto silica nanoparticles. For these experiments, the temperature, the time and the initial concentration are respectively equal to  $60^\circ\text{C}$ , 2 h and 10 %

### 3.2.2. The Effect of silane concentration

These experiments were carried out at pH 3 with a treatment time of 2 h at  $60^\circ\text{C}$ . The extent of recovery was determined using the dissolution test previously mentioned. The amount of silane bonded permanently to the surface of the silica nanoparticles,  $C_b$ , can be calculated by determining its concentration in the solution obtained from this process. After a first linear section, the correlation of the amount used for the treatment ( $C_t$ ) and the silane bonded ( $C_b$ ) tends to converge to the saturation. The characteristic quantities which can be derived from the

correlation are: the proportionally bonded silane,  $C_{100}$ , and the saturation value,  $C_{\max}$ , i.e., the maximum amount of silane that can be bonded to the surface under the grafting conditions [37,43].

Figure 8 presents the dissolution curve of AEAPTMS for which a linear part can be distinguished where the adsorbed amount is proportional to the initial concentration, currently designated as  $C_{100}$ . In the horizontal part of this curve, the adsorbed amount does not vary with the initial concentration. In this case, the maximum amount of silane can be adsorbed in the surface is noted as  $C_{\max}$ . The results obtained show that the adsorbed amounts on the silica surface increase rapidly up to the concentration of 6%. Then, this increase becomes slower until the maximum recovery reaches a value of  $C_{\max}$  close to 6.56%. This result reflects a rapid interaction between AEAPTMS and the surface of silica and after that the interaction takes place more slowly reaching an equilibrium between the surface on which the silane is adsorbed and the free silane existing in the solution.

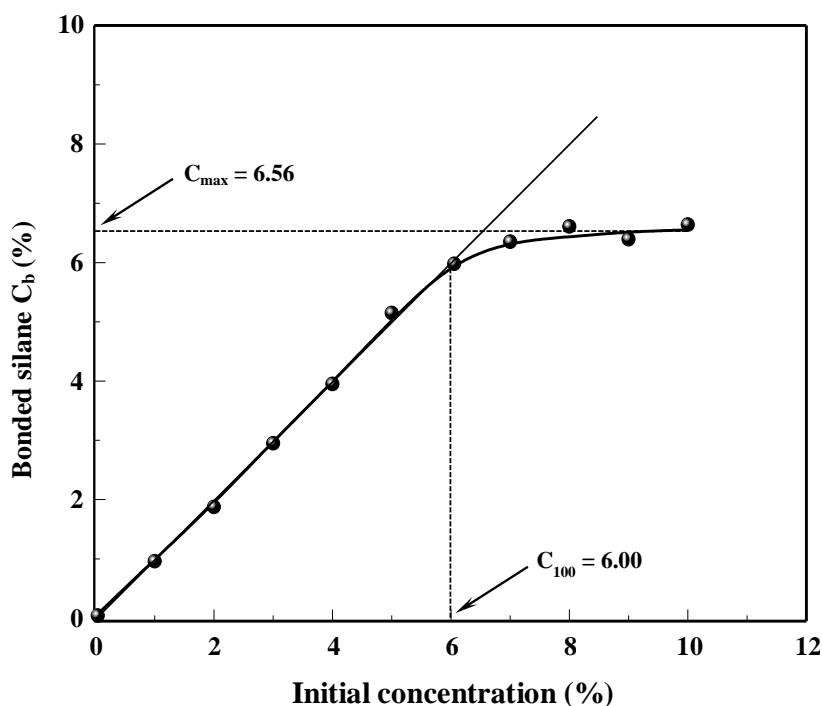


**Fig.8.** Effect of initial concentration on the adsorption of AEAPTMS onto silica nanoparticles. For these experiments, the temperature, the pH and the time are respectively 60 °C, 3 and 2 h

The dissolution curve of MPTMS, shown in Figure 9, displays another behavior for which the shape of its curve is comparable to an S-type adsorption isotherm according to the classification

established by Gilles et al. [46]. The typical dissolution curve denotes that the interactions of the MPTMS with silica surface seem to be much more complicated. The characteristic values of  $C_{100}$  and  $C_{\max}$  are 2.98 and 3.0%, respectively.

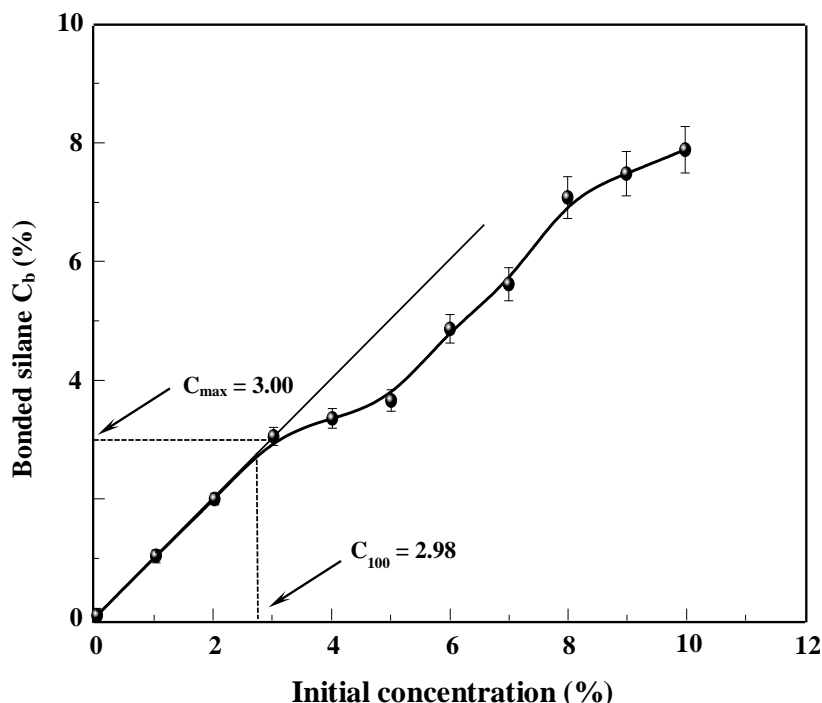


**Fig.9.** Effect of initial concentration on the adsorption of MPTMS onto silica nanoparticles.

For these experiments, the temperature, the pH and the time are respectively 60 °C, 3 and 2 h

The dissolution curve of ATMS presented in Figure 10 is similar to that of MPTMS with the only difference that the first linear section has a greater slope. The corresponding values of  $C_{100}$  and  $C_{\max}$  are 5 and 5.4%, respectively.

Figure 11 illustrates the dissolution curve of CVBS. In this case, three discrete steps are noted, suggesting that the adsorption phenomena are again more complicated. The values of  $C_{\max}$  for each step were found to be 3.2, 5.0 and 6.1%. This result appears as similar to those previously reported by Favis et al. [47] and Doufnoune et al. [43] for the adsorption of CVBS and AEAPTMS on mica flakes and  $\text{CaCO}_3$  surface as a function of treatment time, respectively. For this, it has been proposed that each step (plateau) corresponds to a quantity of silane molecules necessary to create an additional layer of silane on the mica and  $\text{CaCO}_3$  surfaces. If it is considered that the first plateau corresponds to the adsorption of the monolayer, the second and the third one should correspond to a multilayer adsorption. From these curves, it can be



concluded that the adsorbed amount is proportional to the initial concentration until it reaches the maximum value at  $C_{100} = 2.85\%$ .

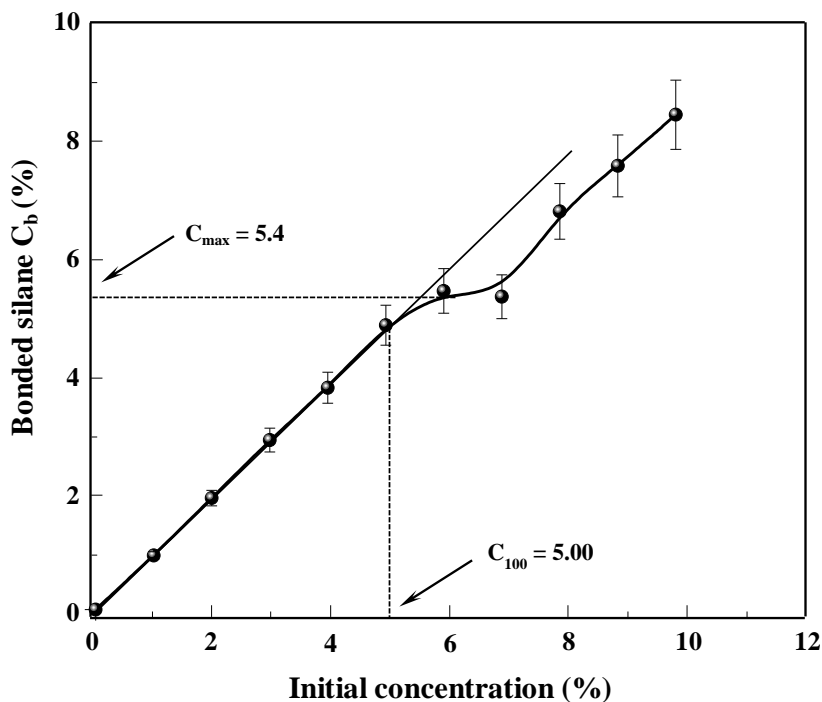


**Fig.10.** Effect of initial concentration on the adsorption of ATMS onto silica nanoparticles.

For these experiments, the temperature, the pH and the time are respectively 60 °C, 3 and 2 h

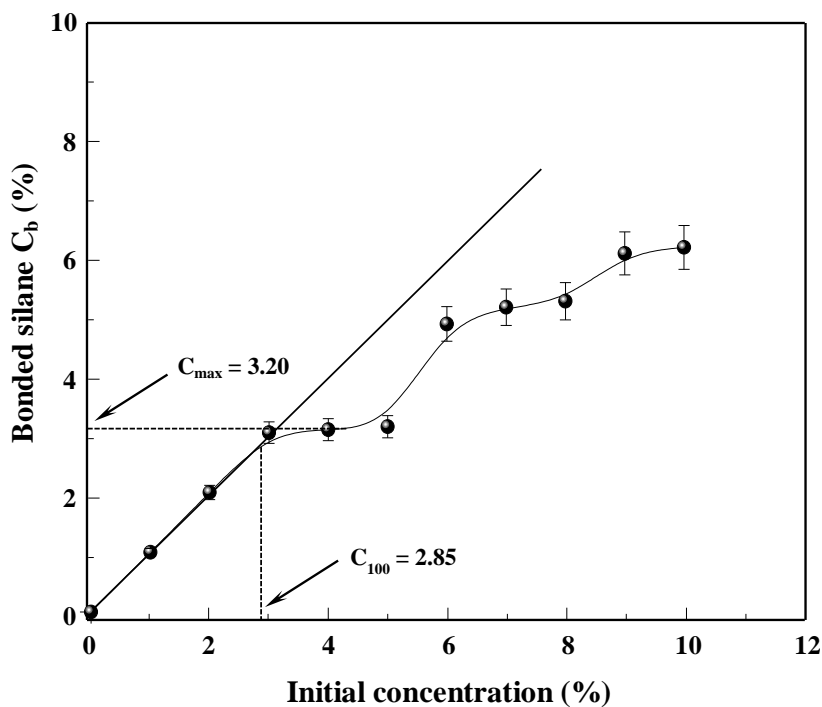


**Fig.11.** Effect of initial concentration on the adsorption of CVBS onto silica nanoparticles.

For these experiments, the temperature, the pH and the time are respectively 60 °C, 3 and 2 h

### 3.2.3. The Effect of treatment time

Figure 12 illustrates the results obtained under the influence of the time effect towards the adsorption treatment with AEAPMS onto silica nanoparticles with two different pH solutions at a temperature of 60 °C and an initial concentration of 10%. Herein, it was observed that under acidic conditions, two discrete steps were noted with a process starting from time zero. The adsorption has grown progressively to reach a first plateau at about 3.7 % while the second was reached at ~ 6.6 % and noted beyond 2 h. In addition, it is observed that under basic conditions, the adsorbed amount reached the plateau only after 2 h and its evolution becomes a monotone function with varying time despite the fact that the process starts also instantly from time zero.

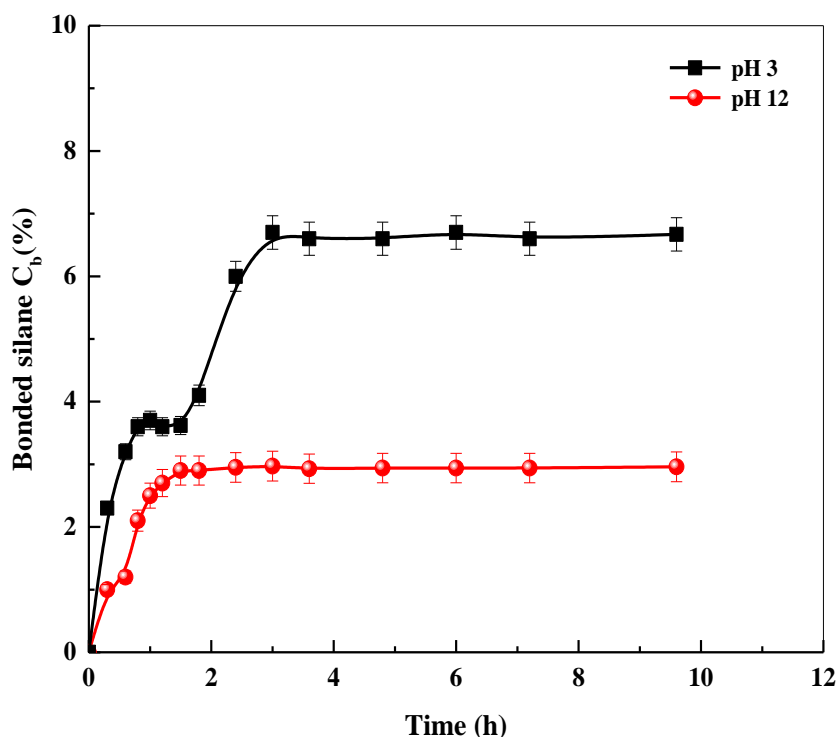


**Fig.12.** Effect of treatment time on the adsorption of AEAPTMS onto silica nanoparticles. For these experiments, the temperature and the initial concentration are respectively equal to 60 °C and 10%

Figure 13 presents the evolution of the adsorption amounts of MPTMS as a function of time. A rapid increase of the adsorbed amount is observed in both acidic and basic conditions. Under the acidic conditions, the adsorbed amount reached the plateau after 3 h and then did

not vary with time whereas in the basic media, a continuous increase in the adsorption amount was observed.

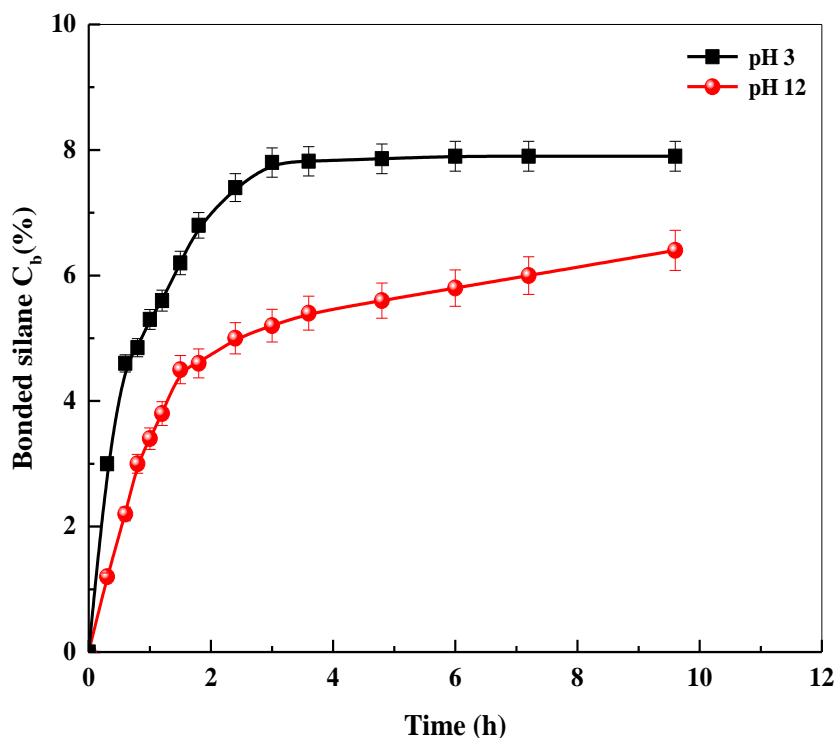


**Fig.13.** Effect of treatment time on the adsorption of MPTMS onto silica nanoparticles. For these experiments, the temperature and the initial concentration are respectively equal to 60 °C and 10%

The variation of adsorption amounts of ATMS with treatment time is given in Figure 14. The adsorption under an acidic environment has revealed that the presence of two plateaus exhibits similarities in the adsorption processes of this molecule with AEAPTMS. The adsorption process starts immediately from time zero and follows a step-like dependence with time. This adsorption increases rapidly at lower values of time reaching the first plateau at about 7.8% after 2.4 h of reaction time. This tendency is almost similar for AEAPTMS, but the final value of the adsorption amount is noticeably higher than that obtained for ATMS even though their respective experiments were performed in the same experimental conditions. The adsorption of ATMS versus the time in basic conditions exhibits three distinct plateaus. The curve obtained showed that the adsorption is increased in a step-wise manner and reached the first plateau at about 2% after 30 min, while the

second and third plateau were reached at about 4 and 4.95% after 3 and 6 h of reaction time, respectively.

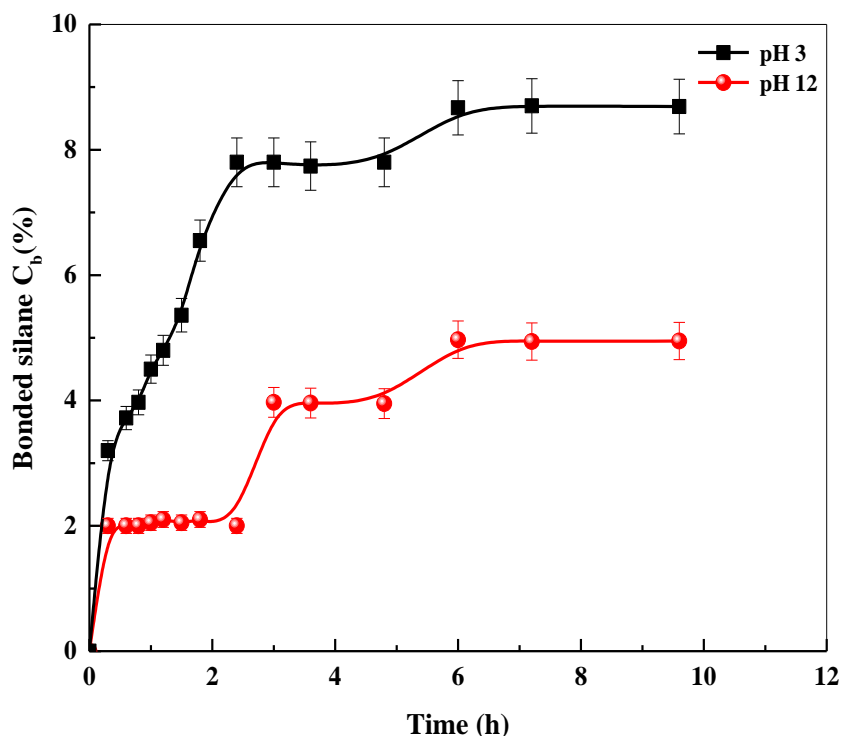


**Fig.14.** Effect of treatment time on the adsorption of ATMS onto silica nanoparticles.

For these experiments, the temperature and the initial concentration are respectively equal to 60 °C and 10%

The evolution of adsorption amount of CVBS onto silica nanoparticles is illustrated in Figure 15. The results obtained showed that the adsorbing silane step-wisely yielded three and two distinct plateaus under acidic and basic conditions, respectively. Under acidic conditions, the adsorption has reached the first plateau at about 3.2% after 1.2 h while the second and third plateau were reached at about 6.0 and 7.9% after 2.4 and 6 h, respectively. Under basic conditions, the amount of CVBS adsorbed reached 2.4 and 3.0% after 1.5 and 2.4 h for the first and the second plateau, respectively. It should also be noted that the silane adsorption onto silica starts instantly from time zero. These results are in perfect agreement with those reported in the literature for the adsorption of CVBS on mica flakes [47].

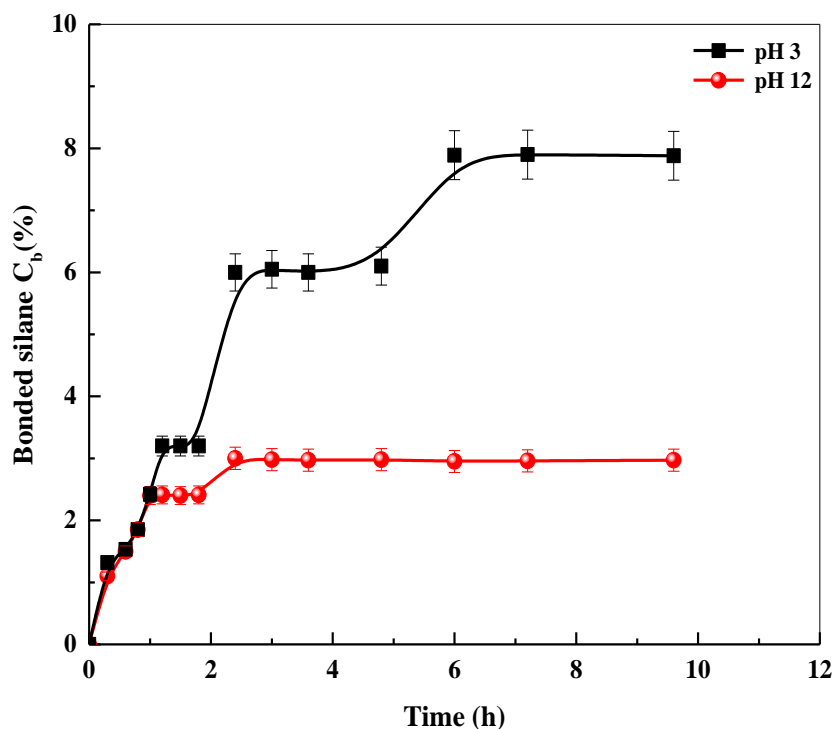


**Fig.15.** Effect of treatment time on the adsorption of CVBS onto silica nanoparticles.

For these experiments, the temperature and the initial concentration are respectively equal to 60 °C and 10%

### 3.2.4. The Effect of the treatment temperature

The influence of the temperature on the silanes adsorption is illustrated in Figure 16. In this case, the surface treatment of silica nanoparticles with different silanes was carried out at different temperatures using 10% of silane solutions judiciously buffered at pH 3 during a period of 2 h. As shown in Figure 16, after a slow increase the amount of adsorption for the four systems rapidly increased up to a maximum level before decreasing.

The optimum absorption amounts appeared at 60 °C, indicating that the modification effect was achieved to the best. The trend of the effect of temperature with all silanes used was similar. This was due to the physical adsorption reaction between silane molecules and the silica surface at lower temperature, rather than effective chemical adsorption. At higher temperatures, the balance of the chemical adsorption reaction converted to the reverse sense, thus the reaction of the silane and silica surface was not efficient.

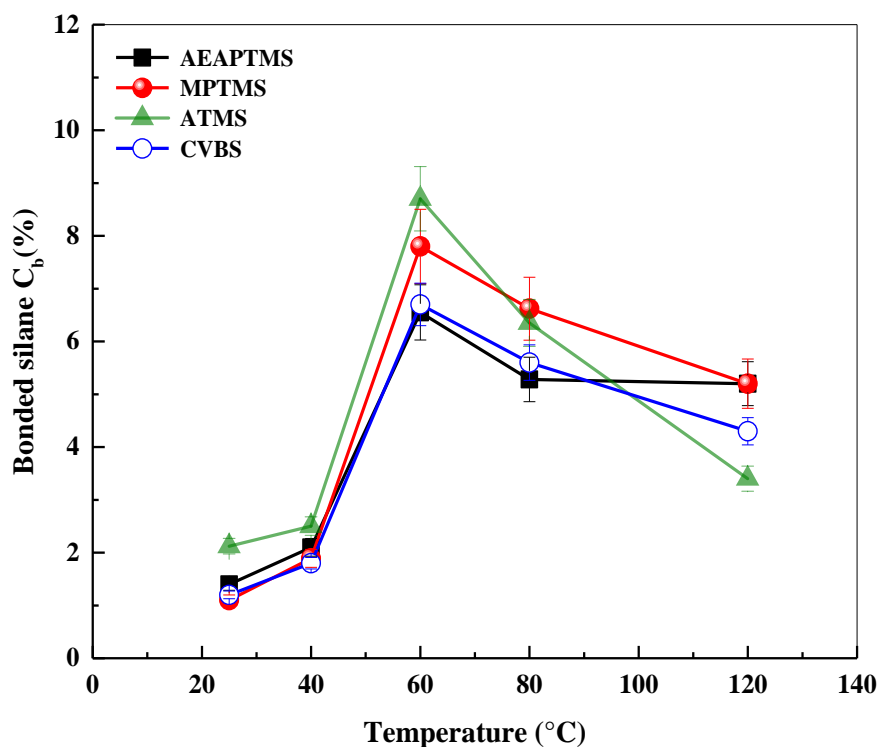


**Fig.16.** Effect of temperature on the adsorption of silanes onto silica nanoparticles. For these experiments, the pH, the time and the initial concentration are respectively equal to 3, 2 h and 10%

#### 4. CONCLUSIONS

Silica nanoparticles were chemically modified in an ethanol/water medium with four silanes compounds; namely: N-(2-Aminoethyl)-3-aminopropyltrimethoxysilane (AEAPTMS), 3-methacryloxypropyltrimethoxysilane (MPTMS), allyltrimethoxysilane (ATMS) and N-2-[(N-vinylbenzylamino)ethyl]-3-aminopropyltrimethoxysilane hydrochloride (CVBS). Effects of the treatment variables including solution pH, silane concentration, reaction time and temperature on the adsorption amounts of silane on the surface of silica were investigated using the dissolution test and FT-IR spectroscopy. The results showed chemical interactions between different silanes and silica nanoparticles. Also, the adsorption of silanes on the silica surface was found to be dependent and greatly sensitive to the initial concentration of the treating solution, treatment time and temperature.

## 5. REFERENCES

- [1] Park SK, Kim KD, Kim HT. Preparation of silica nanoparticles: determination of the optimal synthesis conditions for small and uniform particles colloids surf. Int. J. A. Physicochem. Eng. Asp., 2002, (197), 7-17.
- [2] Lauriente D, Yokose K. Chemical Economics. Handbook; 2005.
- [3] Payne C.C. The Colloid chemistry of silica. Wilmington (Eds.), Advances in Chemistry: American Chemical Society, 1994, pp. 581-594.
- [4] Kang S, Hong SI, Choe CR, Park M, Rim S, Kim J. Preparation and characterization of epoxy composites filled with functionalized nanosilica particles obtained via sol-gel process. Int. J. Polymer, 2001, (42), 879-887.
- [5] Preghenella M, Pegoretti A, Migliaresi C. Thermo-mechanical characterization of fumed silica-epoxy nanocomposites. Int. J. Polymer, 2005, (46), 12065-12072.
- [6] Schick MJ, Hubbard T. Colloidal silica fundamentals and applications. Taylor & Francis Group (Eds). California (C): 2006, pp. 157-176.
- [7] Legrand A, Hommel H, Tuel A, Vidal A, Balard H, Papirer E, Levitz P, Czernichowski M, Erre R, and Damm H. Hydroxyls of silica powders. Adv Colloid Interface Sci., 1990, (33), 291-330.
- [8] Nakamura Y, Yamazaki R, Fukuda T, Shitajima K, Fujii S, and Sasaki M. Structure of silane layer formed on silica particle surfaces by treatment with silane coupling agents having various functional group. Int. J. Adhes Sci Technol., 2014, (28), 1895-1906.
- [9] Iler RK. The chemistry of silica. John Wiley & Sons. New York (NY): 1979, p. 667.
- [10] Zhuravlev L. The surface chemistry of amorphous silica colloids surf. Int. J. Physico-Chem Eng Asp., 2000, (173), 1-38.
- [11] Morrow B, Farlen M. Chemical reactions at silica surfaces. Int. J. Non-Cryst Solids., 1990, (120), 61-71.
- [12] Vansant E F, Van der Voort P, Vrancken K C. Quantification of silanol number in characterization and chemical modification of the silica surface. Amsterdam (Netherlands): E.S.B.V (Eds.), 1995, p. 79-91.

- 
- [13] Rosch L, John P, Reitmeier R. Silicon compounds, organic. Germany: Ullmann's Encyclopedia of industrial chemistry (Eds), 1997, pp. 21-23.
- [14] Plueddemann E. Interfaces in polymer matrix composites. Academic press. New York (NY): 1974. pp. 31-77.
- [15] Osterholtz F, Pohl E. Kinetics of the hydrolysis and condensation of organofunctional alkoxy silanes. *Int. J. Adhes Sci Technol.*, 1992, (6), 127-149.
- [16] Okabayashi H, Shimizu I, Nishio E, and O'Connor C. Diffuse reflectance infra-red Fourier-transform spectral study of the interaction of 3-aminopropyltriethoxysilane on silica gel. Behavior of amino groups on the surface. *Int. J. Colloid Polym Sci.*, 1997, (275), 744-753.
- [17] Yee J, Parry D, Caldwell K, and Harris J. Modification of quartz surfaces via thiol-disulfide interchange. *Int. J. Langmuir*, 1991, (7), 307-313.
- [18] Mercier L, Pinnavaia T. Access in mesoporous materials: advantages of a uniform pore structure in the design of a heavy metal ion adsorbant for environmental. *Int. J. Adv Mater.*, 1997, (9), 500-503.
- [19] Kim J, Seidler P, Wan L, and Fill C. Formation, structure, and reactivity of amino-terminated organic films on silicon substrates. *Int. J. Colloid Interface Sci.*, 2009, (329), 114-119.
- [20] Ciampi S, Harper J, Gooding J. Wet chemical routes to the assembly of organic monolayers on silicon surfaces via the formation of Si-C bonds: Surface preparation, passivation and functionalization. *Int. J. Chem Soc Rev.*, 2010, (39), 2158-2183.
- [21] Gooding J, Ciampi S. The molecular level modification of surfaces: From self-assembled monolayers to complex molecular assemblies. *Int. J. Chem Soc Rev.*, 2011, (40), 2704-2718.
- [22] Haensch C, Hoepfner S, Schubert U. Chemical modification of self-assembled silane based monolayers by surface reactions. *Int. J. Chem Soc Rev.*, 2010, (39), 2323-2334.
- [23] Suzuki N, Ishida H. A review on the structure and characterization techniques of silane/matrix interphases. *Int. J. Macromol Symp.*, 1996, (108), 19-53.
- [24] Boukherroub R, Morin S, Bensebaa F, and Wayner D. New synthetic routes to alkyl monolayers on the Si(100) surface. *Int. J. Langmuir*, 1999, (15), 3831-3835.



- 
- [25] Kim J, Seidler P, Fill C, and Wan L. Investigations of the effect of curing conditions on the structure and stability of amino-functionalized organic films on silicon substrates by Fourier transform infrared spectroscopy, ellipsometry, and fluorescence microscopy. *Int.J. Surf Sci.*, 2008, (602), 3323–3330.
- [26] Kluth G, Sung M, Maboudian R. Thermal behavior of alkylsiloxane self-assembled monolayers on the oxidized Si(100) surface. *Int.J. Langmuir*, 1997, (13), 3775–3780.
- [27] Asay D, Kim S. Evolution of the adsorbed water layer structure on silicon oxide at room temperature. *Int. J. Phys Chem B.*, 2005, (109), 16760–16763.
- [28] Vandenberg E, Bertilsson L, Liedberg B, Uvdal K, Erlandsson R, Elwing H, and Lundström I. Structure of 3-aminopropyltriethoxy silane on silicon oxide. *Int. J. Colloid Interface Sci.*, 1991, (147), 103–118.
- [29] Monredon-Senani S. Interaction organosilanes/silice de precipitation du milieu hydro-alcoolique au milieu aqueux. University Paris VI; 2004
- [30] Wasserman S, Tao Y, Whitesides G. Structure and reactivity of alkylsiloxane monolayers formed by reaction of alkyltrichlorosilanes on silicon substrates. *Int.J. Langmuir*, 1989, (5), 1074-1087.
- [31] Tripp C, Hair M. Reaction of methylsilanols with hydrated silica surfaces: the hydrolysis of trichloro-, dichloro and monochloromethylsilanes and the effects of curing. *Int.J. Langmuir*, 1995, (11), 149-155.
- [32] Peeters M. An NMR study of MeTMS based coatings filled with colloid silica. *Int. J. Sol-Gel Sci Technol.*, 2000, (19), 131-135.
- [33] Behringer K, Blümel I. Reactions of ethoxysilanes with silica: a solid state NMR study. *Int. J. Liq Chromatogr Related Technol.*, 1996, (19), 2753-2765.
- [34] Hoh K, Ishida H, Koenig J. Spectroscopic studies of the gradient in the silane coupling agent/matrix interface in fiberglass-reinforced epoxy. *Int.J. Polym Compos.*, 1988, (9), 151–157.
- [35] Ikuta N, Maekawa Z, Hamada H, Ichihashi M, and Nishio E. Evaluation of interfacial properties in glass fibre-epoxy resin composites – reconsideration of an embedded single filament shear-strength test. *Int. J. Mater Sci.*, 1991, (26), 4663-4666.

- 
- [36] Yi H, Linxia G, Sundaralingam P, and Xiaodong Z. Role of interphase in the mechanical behavior of silica/epoxy resin nanocomposites. *Int. J. Materials*, 2015, (8), 3519-3531.
- [37] Demjen Z, Pukanszky B, Foldes E, and Nagy J. Interaction of silane coupling agents with CaCO<sub>3</sub>. *Int. J. Colloid Interface Sci.*, 1997, (190), 427-436.
- [38] Migliorini S. Agent de couplage et surfaces modèles de silice, suivi en infrarouge ATR du greffage d'organosilanes sur oxyde de silicium. University of Montpellier II; 2000.
- [39] Culler S, Ishida H, Koenig J. FT-IR characterization of the reaction at the silane/matrix resin interphase of composite materials. *Int. J. Colloid Interface Sci.*, 1986, (109), 1-10.
- [40] Dibyendu S, Rama Dubey N, Zhang J, Xie V, Varadan D, and Mathur G. Chemical functionalization of carbon nanotubes with 3-methacryloxypropyl-trimethoxysilane (3-MPTS). *Int. J. Smart Mater Struct.*, 2004, (13), 1263–1267.
- [41] Colon H, Zhang X, Murphy J, Rivera J, and Colon L. Allyl-functionalized hybrid silica monoliths. *Int. J. Chem Commun.*, 2005, (22), 2826–2828.
- [42] Chiang C, Ishida H, Koenig J. The structure of  $\gamma$ -aminopropyltriethoxysilane on glass surfaces. *Int. J. Colloid Interface Sci.*, 1980, (74), 396–404.
- [43] Doufnoune R, Haddaoui N, Riahi F. The Interactions of silane and zirconate coupling agents with calcium carbonate. *Int. J. Polymer Mater.*, 2007, (56), 227–246.
- [44] Ishida H, Koenig J. Fourier transform infrared spectroscopic study of the structures of silane coupling agent on E-glass fiber. *Int. J. Colloid Interface Sci.*, 1978, (64), 565-576
- [45] Bellamy LJ. *The Infrared spectra of complex molecules*. John Wiley & Sons (Eds). New York (NY): 1975. pp. 236-238.
- [46] Gilles C, McEvan T, Nakhauva S, and Smith D. A system of classification of solution adsorption isotherms, and its use in diagnosis of adsorption mechanisms and in measurement of specific surface areas of solids. *Int. J. Chem Soc.*, 1960, 3973-3993.
- [47] Favis B. The formation of coupling agent monolayers on the surface of mica. *Int. J. Polym Compos.*, 1984, (5), 11-17.
- [48] Plueddemann E. Principles of interfacial coupling in fibre-reinforced plastics. *Int. J. Adhes Adhes.*, 1981, (1), 305–310.

[49] Minhong X, Yongyong C, Shunguo G. Surface modification of nano-silica with silane coupling agent. *Int. J. Key Eng Mater.*, 2015, (636), 23-27.

**How to cite this article:**

Bounekta O, Doufnoune R, Ourari A, Riahi F, Haddaoui N. Surface modification of silica nanoparticles by means of silanes: effect of various parameters on the grafting reactions. *J. Fundam. Appl. Sci.*, 2019, *11(1)*, 200-226.